Journal of Electroceramics 2:3, 151–156, 1998

A Novel Oxygen Sensor Based on a Metal–Metal Oxide Scale System

KEN-ICH KAWAMURA, ATSUSHI KAIMAI, YUTAKA NIGARA, TATSUYA KAWADA & JUNICHIRO MIZUSAKI

Research Institute for Scientific Measurements, Tohoku University, 2–1–1 Katahira, Aoba-ku, Sendai 980-8577, Japan

Submitted July 7, 1997; Revised May 14, 1998; Accepted May 14, 1998

Abstract. A novel oxygen sensor was proposed. The sensor, an electrochemical cell, was composed of a metal as reference electrode, its oxide scale as electrolyte and Pt or other adequate materials as sample electrode. It is expected that the electrolyte is self-restorative because it can be restored by high temperature oxidation. The emf measurements were carried out at 873 K in cells using zirconium. At $P_{O_2} = 1 \sim 10^{-3}$ atm, the emf vs. $\log P_{O_2}$ plot lies on a straight line and its gradient is $2.303RT/4F$, suggesting $t_{ion} = 1$ at the surface of the scale. The emf steeply decreases with decreasing P_{O_2} at $P_{O_2} < 10^{-3}$ atm which can not be explained by the increase in the electronic conductivity and is explained by a gas laminar film phase at the surface of the sample electrode.

Keywords: self-restoration of the electrolyte, high temperature oxidation, Zr, electromotive force

1. Introduction

In the high temperature oxidation of metals, an oxygen potential gradient is formed in the scale [1]. If the growth rate of the scale is determined by a diffusion process in the oxide scale, the oxygen potential gradient is uniquely determined by the oxygen partial pressures of the gas phase, $P^{I}_{O_2}$, and at the interface between metal and oxide scale, $P^{II}_{O_2}$ (Fig. 1). If an adequate electrode (AE) is applied to the scale surface, the metal and its oxide scale constitute a solid electrochemical cell as;

$$\text{Metal, } P^{II}_{O_2} \mid \text{Oxide scale} \mid \text{AE, } P^{I}_{O_2} \qquad (1)$$

When the scale has enough ionic conductivity, an electromotive force (emf) is induced between the metal and the scale surface. The emf, E, is represented by

$$E = \frac{RT}{4F} \int_{\ln P^{II}_{O_2}}^{\ln P^{I}_{O_2}} t_{ion} \mathrm{d} \ln P_{O_2} \qquad (2)$$

where T is the temperature, F is the Faraday constant, R is the gas constant, and t_{ion} is the ionic transference number in the oxide scale [2]. $P^{II}_{O_2}$ can be considered as the equilibrium oxygen partial pressure between the metal and the oxide, which only depends on temperature. When the temperature is given, the emf is a function of $P^{I}_{O_2}$ and t_{ion}. Therefore, if t_{ion} is known, the metal and its oxide scale may serve as an oxygen sensor.

It is necessary to chose a metal in cell (1) for which the oxide scale is formed by inward diffusion of oxygen. When the scale is grown by outward diffusion of the cation, the outer electrode becomes embedded inside the scale (the electrode functions as a marker).

Figure 2 compares oxygen sensors, a) using a metal and its oxide scale and b) using stabilized ZrO_2. Using the oxide scale as the electrolyte, it is expected that the cell may have the following advantages.

- self-restoration of the electrolyte
- easy to manufacture

When the scale is broken, it is repaired by oxidation of the metal leading to flexibility in treatment. Considering cell (1) as a sensor for measuring the oxygen content in a liquid metal, the sensor would be constructed simply by inserting the metal with the oxide scale and the AE, such as

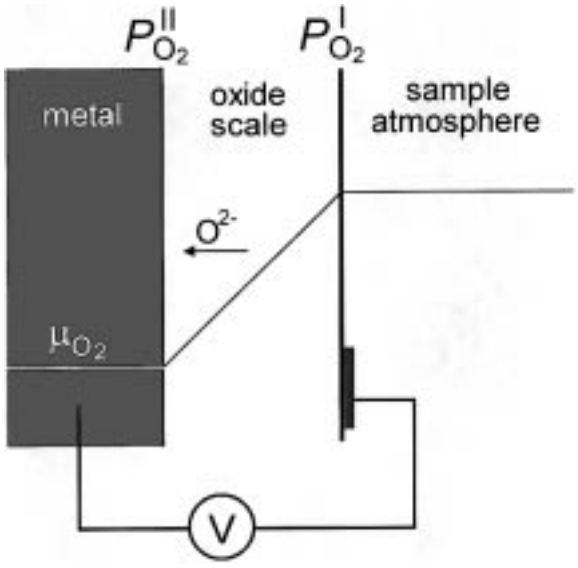

Fig. 1. Schematic diagram of oxide scale.

$LaCrO_3$, in the liquid metal without further preparation.

In the present study, a novel cell of the type in Eq. (1) is proposed, and the properties are discussed in relation to the oxidation behavior.

2. Theory

To obtain the emf of the cell as a function of $P^{I}_{O_2}$, we must select the metal and scale in which $t_{ion} \sim 1$ at the scale surface near the sensing atmosphere. In this section, the emf of the cell for a specific case is considered.

The emf of the cell is calculated by integration of t_{ion} from $\ln P^{I}_{O_2}$ to $\ln P^{II}_{O_2}$. Assuming $t_{ion} = 1$, Eq. (2) becomes the Nernst equation:

$$E = \frac{RT}{4F} \ln \frac{P^{I}_{O_2}}{P^{II}_{O_2}} \tag{3}$$

Equation (3) is well known as the equation of the emf of an oxygen concentration cell such as in a stabilized ZrO_2 oxygen sensor. However, it is difficult to assume that t_{ion} is unity throughout the oxide scale from the metal/oxide interface to the oxide/gas interface because the electronic conductivities are dependent on oxygen deficiency or excess caused by the variation in the oxygen partial pressures. Defect chemical models are known to predict that ionic conductors show hole conduction under high oxygen partial pressures and electronic conduction under low ones (Fig. 3(a)). When $P^{II}_{O_2}$ is in the region of $t_{ion} \cong 0$, (Fig. 3(b)), the emf may change as in Fig. 3(c) [3]. At the region of $P^{I}_{O_2}$ corresponding to $t_{ion} = 1$, the plot of the emf and the value calculated from Eq. (3) against $\log P^{I}_{O_2}$ are in parallel.

Concerning measurements performed only within the $P^{I}_{O_2}$ region corresponding to $t_{ion} = 1$, it is convenient to define an oxygen partial pressure of P_{ec} by the following equation

$$\int_{\ln P_{ec}}^{\ln P^{I}_{O_2}} (1 - t_{ion})\, \mathrm{d}\ \ln\ P_{O_2} = \int_{\ln P^{II}_{O_2}}^{\ln P_{ec}} t_{ion}\, \mathrm{d} \ln P_{O_2} \tag{4}$$

where we assumed $t_{ion} = 1$ at $P^{I}_{O_2}$. Then, P_{ec} corresponds to the oxygen partial pressure at the cross point between $E = 0$ and extrapolated line from the region of $t_{ion} = 1$ in Fig. 3(c). Under the condition of $P^{II}_{O_2} \ll P_{ec} \ll P^{I}_{O_2}$, Eq. (2) is represented by

$$E = \frac{RT}{4F} \ln \left(\frac{P^{I}_{O_2}}{P_{ec}} \right) \tag{5}$$

Therefore, when we select a metal with the oxide scale satisfying $P^{II}_{O_2} \ll P_{ec}$, the emf of the cell (1) would not depend on $P^{II}_{O_2}$.

3. Experimental

In cell (1), the scale must be an ionic conductor which grows by inward diffusion of oxygen. Pure zirconium was chosen as the metal substrate, because its oxide, ZrO_2, is the most popular oxide ion conductor when containing dopants such as CaO, Y_2O_3 or MgO to stabilize the CaF_2 structure.

Specimens were made of zirconium wire (ϕ1.0 mm, 99.5% purity) purchased from Nilaco Co. Japan. The end of the wire was wound onto a stick (ϕ8 mm) 10 times and onto itself 8 times to increase the surface area and the other part of the wire was used as an anode leadout (Fig. 4). A surface of the coiled Zr was oxidized in air at 973 K for about 60 s (1 min) to form an oxide scale as an electrolyte. Pt paste, which worked as cathode, was painted on the surface of the scale and fired at 1073 K for about 120 s (2 min) under O_2 flow. The construction of the test cell was as follows.

$$\mathrm{Zr(metal)} \mid \mathrm{ZrO_2(oxide\ scale)} \mid \mathrm{Pt},\ P^{I}_{O_2} \tag{6}$$

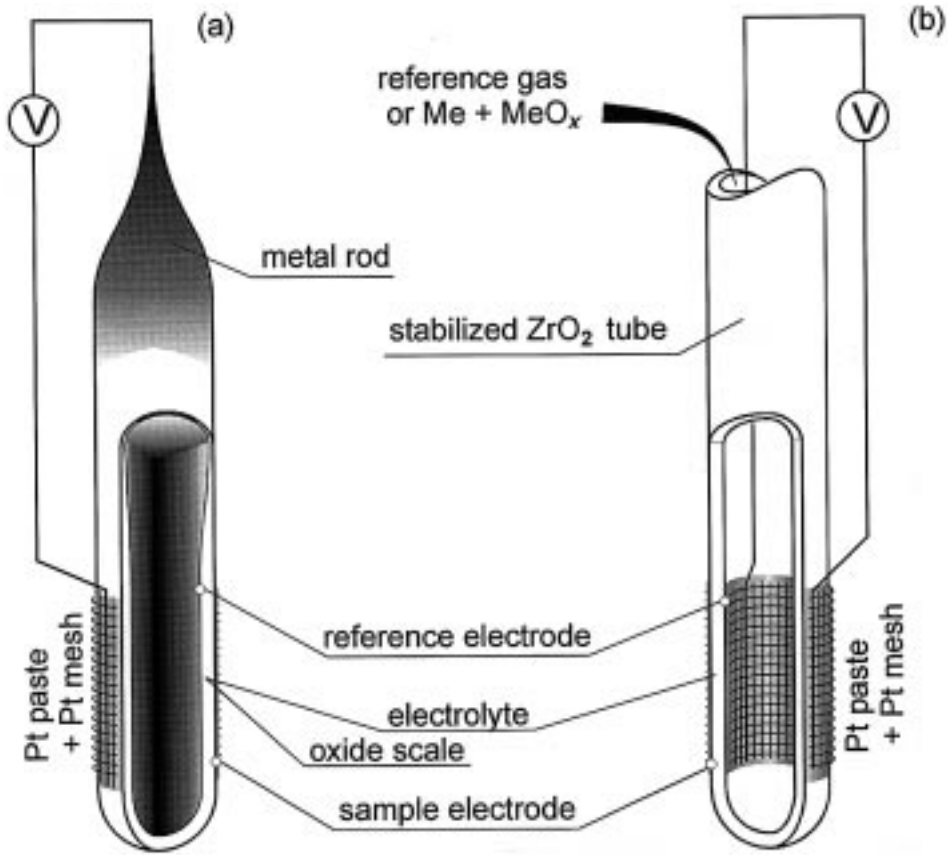

Fig. 2. Schematic diagram of oxygen sensors using a metal and its oxide (a), and using stabilized zirconia (b).

To insure the reproducibility and enable the study of the influence of gas flow rate, another type of cell was prepared as shown in Fig. 2. A Pt wire was directly wound onto a straight zirconium wire without pre-oxidation.

The emf measurements were made at 873 K under controlled oxygen partial pressure ($1 \sim 10^{-5}$ atm) using Ar–O_2 gas mixtures. The emf was measured using an electrometer with an input impedance of $10^{12}\Omega$. After emf measurements, the scale surface was observed by the microscope and its structure was confirmed by powder X-ray diffraction.

4. Result and Discussion

Figure 5 shows the emf of the test cell as a function of oxygen partial pressure at 873 K. The different symbols indicate the emf on increasing and decreasing $P^{\mathrm{I}}_{\mathrm{O}_2}$. The open and solid symbols mean different runs. The emf values can be divided into two regions.

Under oxygen partial pressures higher than 10^{-4} atm, the emf lies on a straight line. The least squares fit gives the emf by the following expression.

$$E/\mathrm{V} = 1.32 + 4.33 \times 10^{-2} \ \log(P^{\mathrm{I}}_{\mathrm{O}_2}/\mathrm{atm}) \qquad (7)$$

From Eq. (2), the gradient of the emf corresponds to the ionic transference number at the surface of the oxide scale. The gradient of the emf is close to $2.303RT/4F$, suggesting $t_{\mathrm{ion}} \approx 1$.

By using Eq. (5), P_{ec} is calculated from the emf as shown in Fig. 5. The value of P_{ec} is constant and equal to $10^{-30.6}$ atm.

Let us compare our results assumed for undoped ZrO_2 with those expected for stabilized ZrO_2. At low oxygen partial pressures, defect equilibrium in stabilized ZrO_2 can be written as follows.

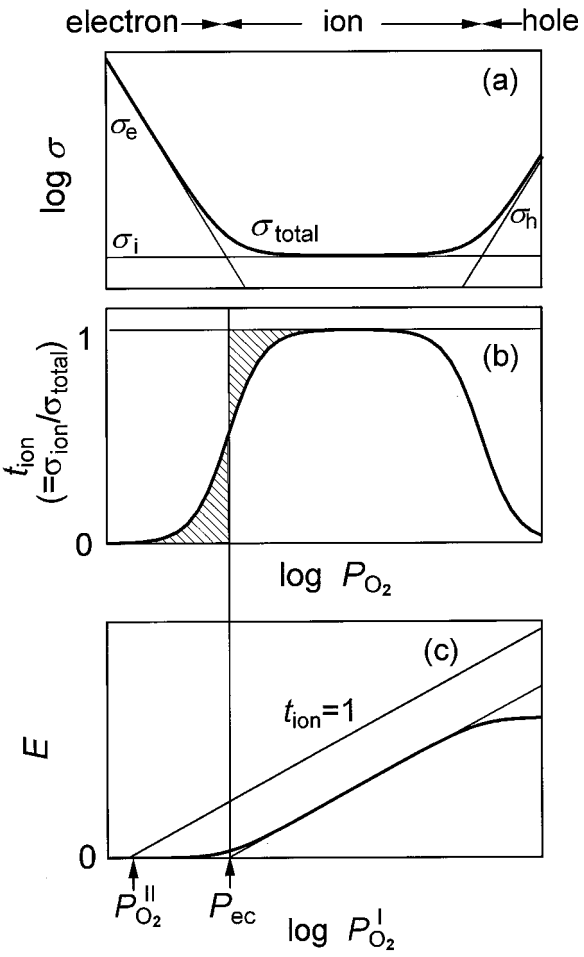

Fig. 3. Schematic diagram of dependence on oxygen partial pressure of conductivity (a), ionic transference number (b) and emf (c).

$$O_O^{\times} = \frac{1}{2}O_2 + V_O^{\cdot\cdot} + 2e' \tag{8}$$

There is a large concentration of vacancies in stabilized ZrO_2 due to doping. Therefore, the concentration of oxygen vacancies, $[V_O^{\cdot\cdot}]$, is regarded as constant. The dilute solution model may be applied, because the equilibrium concentration of electrons is very small. Then it follows from Eq. (8) that the concentration of electrons varies as $P_{O_2}^{-1/4}$. When the mobility of the electron is independent of the oxygen partial pressure, the total conductivity is given by

$$\sigma_{total} = \sigma_{ion} + \sigma_e^{\circ} P_{O_2}^{-1/4} \tag{9}$$

where σ_e° is the electronic conductivity at $P_{O_2} = 1$ atm. In stabilized ZrO_2, a partial electronic conduction parameter, P_e, is defined as the oxygen pressure at which the ionic and the electronic conductivities are equal [5,6]. Using these definitions, the emf is represented by

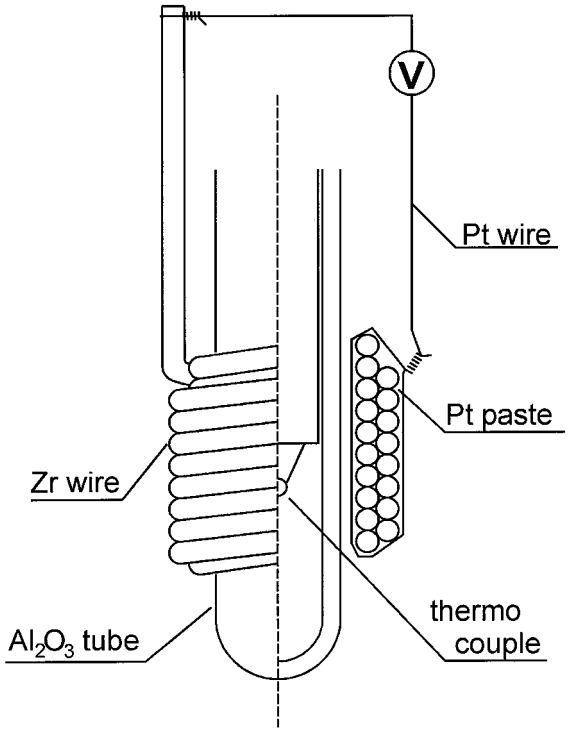

Fig. 4. Schematic illustration of the cell.

$$E = \frac{RT}{F}\ln\frac{P_e^{1/4} + P_{O_2}^{I\ 1/4}}{P_e^{1/4} + P_{O_2}^{II\ 1/4}} \tag{10}$$

If Eq. (9) holds in the present study, P_{ec} is close to P_e. Figure 5 includes P_e of 11 mol% CaO stabilized ZrO_2 extrapolated from the values determined by the emf method [3]. The present P_{ec} is about ten orders higher than P_e. The assumption of Eq. (9) is valid when the sample contains impurity elements to stabilize the CaF_2 structure in the ZrO_2 oxide scale and/or the oxide scale has a large amount of oxygen vacancies caused by thermal activation. Therefore the difference between P_{ec} and P_e is reasonable, because the oxide scale is essentially pure ZrO_2 which contains no stabilizer, and is considered to show much lower ionic conductivity than stabilized ZrO_2.

Under oxygen partial pressures lower than 10^{-4} atm, a decrease in oxygen partial pressure causes a steep decrease in the emf. The slope of the emf

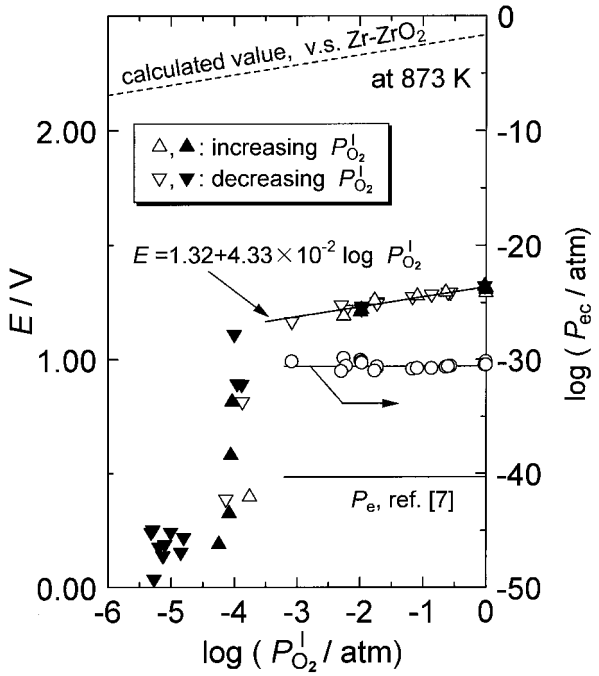

Fig. 5. Emf of the test cell and P_{ec} as a function of the oxygen partial pressure, $P^{I}_{O_2}$. P_e is the extrapolated value for 11 mol% CaO stabilized ZrO_2 [3]. The dotted line shows calculated emf using the equilibrium oxygen pressure of Zr–ZrO_2 [4].

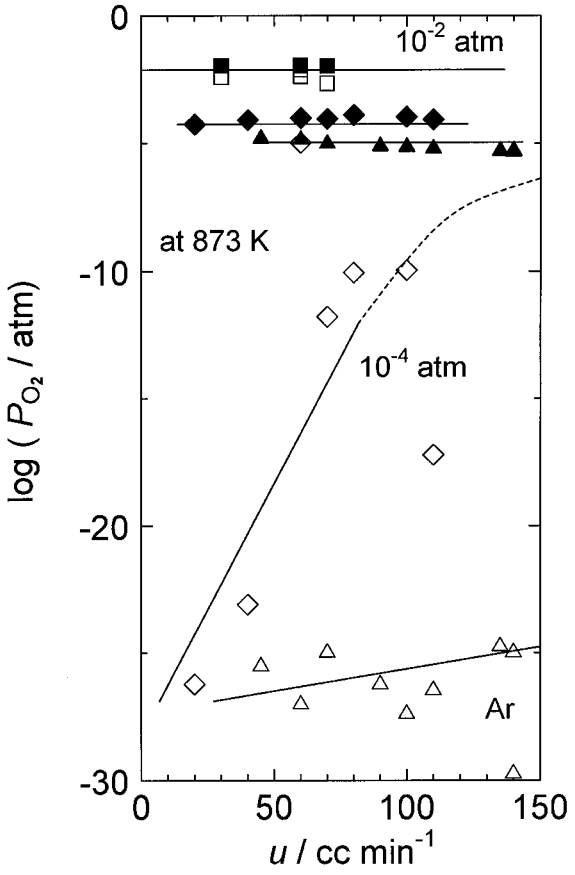

Fig. 6. Flow rate dependence on the oxygen partial pressure from the emf of the test cell (open marks) and from an oxygen sensor after the test cell (solid marks), □ Ar–10^{-2} O_2, Ar–10^{-4} O_2, pure Ar (upper limit of P_{O_2} is 10^{-5} atm).

indicates $t_{ion} \gg 1$. Since the value of t_{ion} can not theoretically exceed 1, the steep decrease in emf can not be caused by changes in transference numbers.

Based on Eq. (5), the emf depends directly upon the values of $P^{I}_{O_2}$ and P_{ec}. P_{ec} is only determined by the electrical properties of the oxide and the temperature. It is suggested that the steep decrease in emf is caused by a decrease of the effective $P^{I}_{O_2}$. The present cell uses the oxide scale as the electrolyte. The scale when growing exhausts the oxygen. Therefore, when the oxygen consumption rate due to oxidation is not negligible relative to the amount of inlet oxygen gas, it is possible that the oxygen partial pressure around the scale surface is lower than that of the introduced gas. If this hypothesis is true, the emf should show a dependence on the gas flow rate.

Figure 6 shows the oxygen partial pressure calculated by Eq. (5) by using the emf of the test cell with $P_{ec} = 10^{-30.6}$ atm as a function of gas flow rate, u, and from a stabilized ZrO_2 oxygen sensor placed after the test cell. Using an Ar–O_2 premixed gas with $P_{O_2} = 10^{-2}$ atm, the oxygen partial pressure calculated from the emf of the test cell agreed with that from the emf of the oxygen sensor placed after the cell. There is no dependency on the gas flow rate. When the gas is Ar–O_2 with $P_{O_2} = 10^{-4}$ atm and pure Ar (upper limit of P_{O_2} was 10^{-5} atm), although oxygen partial pressures from the emf of the test cells are scattered, the oxygen partial pressures tend to increase with increasing gas flow rate.

If the steep changes of the emf of the test cells in Fig. 5 are caused by the exhaustion of oxygen by the oxidation of zirconium, the oxygen partial pressure at the exhaust of the cell would agree with that of the emf of the test cells. However, the oxygen partial pressure at the exhaust shows no clear dependency on the gas flow rate. It is considered that the gas practically passes through the furnace without influence on the test cell. This suggests that there is only a gas laminar film on the surface of the test cell.

If a large amount of the gas is supplied to break the gas laminar film phase, the oxygen partial pressure from the emf of the test cell should become closer to the value measured by the oxygen sensor placed after the test cell. That is to say, at the low oxygen partial pressure, it is considered that the emf of the test cell describes the oxygen partial pressure in the gas laminar film phase determined by a competition between the flux of oxygen supplied from the gas flow and that exhausted by oxidation of zirconium.

Figure 7 shows surface of the test cell after the experiment. The surface shows a metallic luster and is covered with Pt-paste which served as an electrode and a marker. It is clear that the oxide scale is grown by inward diffusion of oxygen as already assumed. X-ray diffraction shows that the scale has a monoclinic structure. Although the oxide scale of Zr is not the anion conducting CaF_2 structure at our measuring temperatures, the electrical conductivity is governed by oxide ion conduction in monoclinic ZrO_2 at $P_{O_2} \geq 10^{-3}$ atm.

There are networks of cracks over the oxide scale as shown in Fig. 7. It is believed that the cracks enhance oxidation and decrease the oxygen partial pressure at the gas laminar film phase and degrade the electronic collection of the sample electrode (cathode electrode). To avoid a decrease in the electronic collection, it is necessary to reconsider the design of the electrode or try to measure oxygen in a liquid with electronic conductivity such as liquid metal.

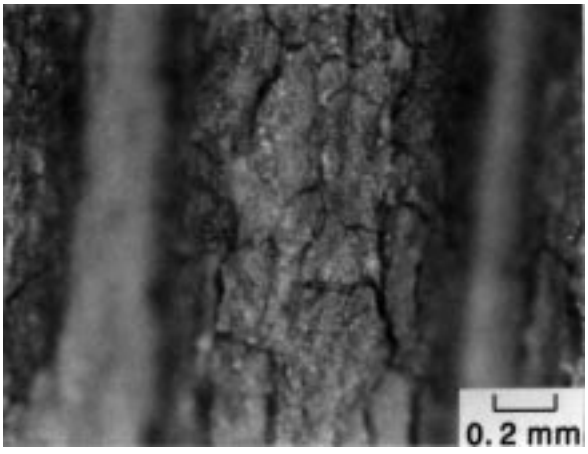

Fig. 7. Optical image of cell surface after the measurement. The surface is covered with Pt-paste that served as electrode and marker.

5. Conclusion

A novel oxygen sensor was proposed, which is composed of a metal and its oxide scale with a sensing electrode attached on the surface of the scale. The emf measurements were carried out with cells using zirconium and Pt as sensing electrode. For $P_{O_2} = 1 \sim 10^{-3}$ atm, the emf vs. $\log P_{O_2}$ plot lies on a straight line and its gradient shows $t_{ion} = 1$ at the surface of the scale. The emf steeply decreases for $P_{O_2} < 10^{-3}$ atm. The steep decrease could not be explained by the change in partial conductivities, but by a gas laminar film phase at the surface of the sample electrode.

References

1. C. Wagner, *Z. Phys. Chem.*, **21**, 25, in German, (1933).
2. C. Wagner, in *Advances in Electrochemistry and Electrochemical Engineering*, Volume 4, edited by P. Delahay (John Wiley & Sons, New York, 1966). p. 1.
3. K. Kawamura, T. Maruyama, and K. Nagata, *Metal. Mater. Trans. B.*, **26B(2)**, 289 (1995).
4. I. Barin, *Thermochemical Data of Pure Substances.* (VCH Publishers, Weinheim, 1989).
5. H. Schmalzried, *Z. Elektrochem.*, **66(7)**, 572 (1962).
6. H. Schmalzried, *Z. Phys. Chem. N. F.*, **38**, 87 (1963).